The Polyphenol Altenusin Inhibits in Vitro Fibrillization of Tau and Reduces Induced Tau Pathology in Primary Neurons

Sook Wern Chua,[†,○] Alberto Cornejo,*[,†,‡,○] Janet van Eersel,[†] Claire H. Stevens,[†] Inmaculada Vaca,[§] Mercedes Cueto,[∥] Michael Kassiou,[⊥] Amadeus Gladbach,[†] Alex Macmillan,[#] Lev Lewis,[#] Renee Whan,[#] and Lars M. Ittner*[,†,∇]

[†]Dementia Research Unit, School of Medical Sciences, Faculty of Medicine, UNSW Australia, Sydney, NSW 2052, Australia
[‡]Faculty of Medicine, Medical Technology School, University Andrés Bello, Sazié 2315, Santiago, Chile
[§]Department of Chemistry, Faculty of Science, University of Chile, Las Palmeras 3425, Ñuñoa, Santiago, Chile
[∥]Institute for Natural Products and Agrobiology CSIC, 38206 La Laguna, Tenerife, Spain
[⊥]School of Chemistry and Faculty of Health Sciences, University of Sydney, Sydney, NSW 2006, Australia
[#]Biomedical Imaging Facility, Mark Wainright Analytical Centre, UNSW Australia, Sydney, NSW 2052, Australia
[∇]Neuroscience Research Australia, Sydney, NSW 2031, Australia

ABSTRACT: In Alzheimer's disease, the microtubule-associated protein tau forms intracellular neurofibrillary tangles (NFTs). A critical step in the formation of NFTs is the conversion of soluble tau into insoluble filaments. Accordingly, a current therapeutic strategy in clinical trials is aimed at preventing tau aggregation. Here, we assessed altenusin, a bioactive polyphenolic compound, for its potential to inhibit tau aggregation. Altenusin inhibits aggregation of tau protein into paired helical filaments in vitro. This was associated with stabilization of tau dimers and other oligomers into globular structures as revealed by atomic force microscopy. Moreover, altenusin reduced tau phosphorylation in cells expressing pathogenic tau, and prevented neuritic tau pathology induced by incubation of primary neurons with tau fibrils. However, treatment of tau transgenic mice did not improve neuropathology and functional deficits. Taken together, altenusin prevents tau fibrillization in vitro and induced tau pathology in neurons.

KEYWORDS: *Microtubule associated protein tau, antiaggregation, Alzheimer's disease*
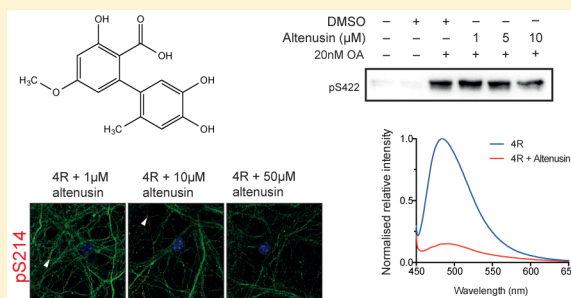
Alzheimer's disease (AD) is the most common form of dementia characterized by senile plaques consisting of amyloid-β (Aβ) and neurofibrillary tangles (NFTs).[1] NFTs are composed of aberrant microtubule-associated protein tau. Under normal physiological conditions, tau binds to microtubules but becomes increasingly phosphorylated in AD. This hyperphosphorylated tau no longer binds to microtubules, but accumulates in the soma and dendrites of neurons, forming intracellular as paired helical filaments (PHFs).[1,2]

Pathological phosphorylation of tau triggers conformational changes that makes it prone to form oligomers.[3−5] Oligomeric tau has been found in tau transgenic mouse models and human AD brains, suggesting a role in the disease.[6,7] Interestingly, improvement in the cognition of a transgenic mouse model displaying both NFTs and senile plaques required the reduction of soluble tau, but not of Aβ plaques.[8,9] Overexpression of tau in neurons has deleterious effects, suggesting intracellular tau aggregates are cytotoxic.[10,11]

Until recently, the major focus of drug development for the treatment of AD has been on Aβ despite a significant number of candidate drugs failing to slow disease progression. For example, immunization against Aβ was effective in reducing amyloid plaque load, but had little effect on cognitive functions in patients.[12−14] In this context, it would be timely to consider alternative drug discovery strategies for AD, including the targeting of misfolded tau.[15,16] Accordingly, developing small-molecule inhibitors of tau aggregation emerged as a strategy for developing new treatments for AD and other tauopathies.[17,18] Some naturally occurring polyphenols have been reported to exhibit antiaggregating effects that prevent amyloid formation[19−21] or tau aggregation, such as cinnamon extract, grape seed, and fulvic acid.[22−25] Furthermore, bacterial- and fungal-derived compounds with anti-tau activities have been reported to possess antitau aggregation properties.[26−28] A benzoquinone macrocyclic polyketide geldamycin isolated from *Streptomyces hygroscopicus* was identified as a Hsp90 inhibitor[3,29] and reported to reduce levels of hyperphosphorylated tau.[30,31]
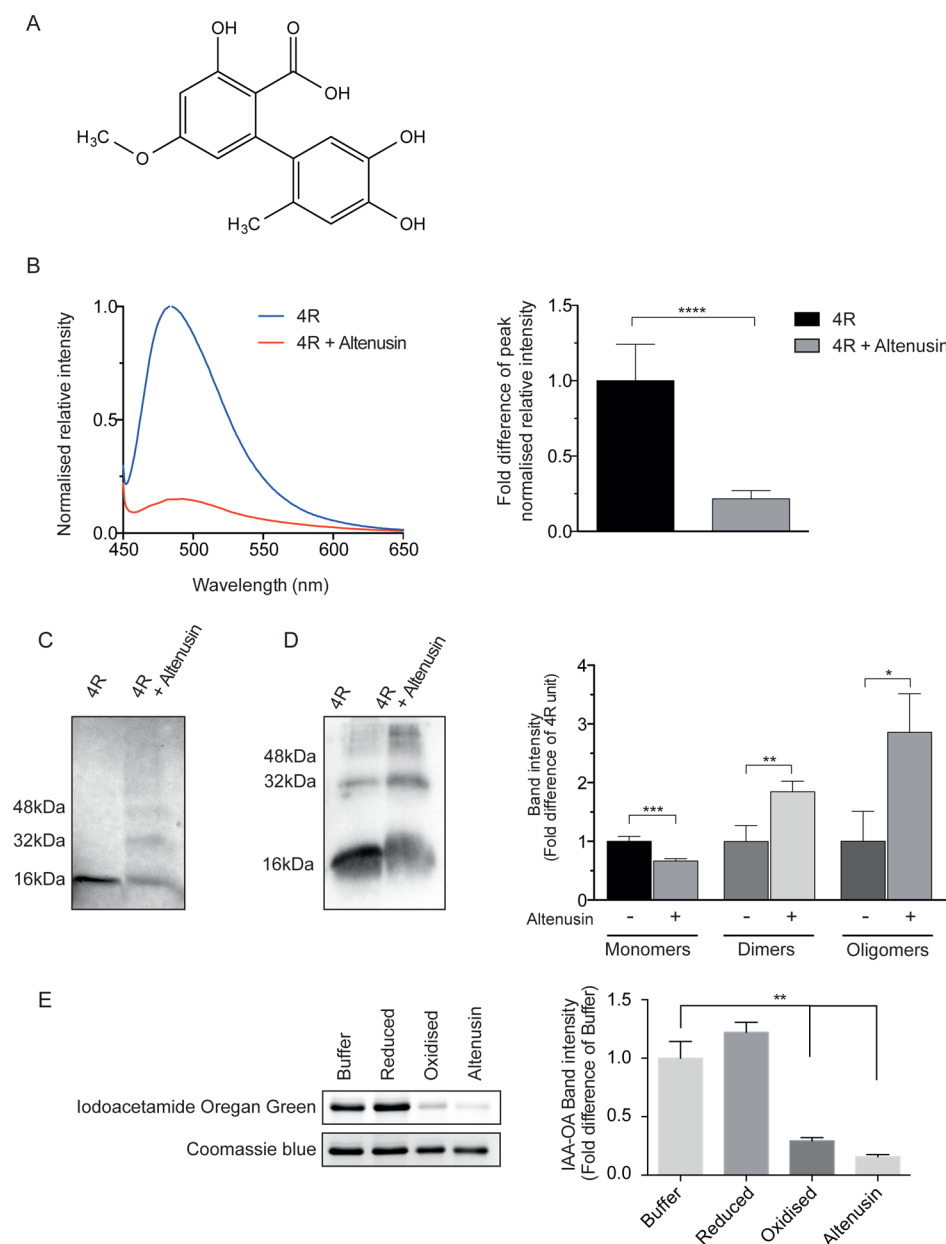
Figure 1. Altenusin inhibits 4R aggregation and stabilizes lower order oligomers. (A) Structure of altenusin. (B) Thioflavin T assay shows a significant decrease ($75.29 \pm 7.3\%$) in fluorescence intensity, indicating a decrease in 4R fibrils in the presence of altenusin. Representative graph from 4 independent experiments is shown (****$P \leq 0.0001$). (C) Coomassie stained gel of the fibrillized 4R preparation show decrease in 4R monomers and an increase in lower order oligomers in the presence of altenusin. (D) Western blots of the 4R preparation used in (B) and (C) show a decrease in 4R monomers and an increase in oligomers. Graph: Quantification of the band intensities from four independent experiments (*$P \leq 0.05$, **$P \leq 0.01$, ***$P < 0.001$). (E) Reduced iodoacetamide-Oregon Green band intensities indicate oxidation of 4R tau. Coomassie blue stained gel shows equal loading. Graph: Quantification of the band intensities from three independent experiments (**$P \leq 0.01$).

Altenusin, a biphenyl polypenolic compound isolated from fungal endophyte *Alternaria* has shown activity against trypanothione reductase and is therefore a drug target for trypanosomatids.[6,32] Here, we investigated the effects of altenusin (Figure 1A) as isolated from *Penicillium* sp. CVAL4 on heparin-induced tau fibrillization and tau phosphorylation in vitro and in vivo. A recombinant four repeat domain tau construct comprising only the microtubule binding domains of tau (amino acids 244−372; referred to as "4R") was used to investigate the effects of altenusin on tau fibril formation. 4R is prone to aggregation and the formation of both straight and paired fibrils consisting of parallel β-sheets,[8,10,33] which can be

monitored by thioflavin-T (ThT) binding to paired helical filaments (PHF).[12,16,34] Notably, tau's N- and C-terminal regions may modulate aggregation,[35] but the 4R region is critical for PHF formation. In the presence of altenusin, heparin-induced polymerization of 4R for 48h was reduced by $75.29 \pm 7.3\%$ compared to 4R alone, as determined by ThT fluorescence spectrum measurement (Figure 1B), indicating a marked reduction in the formation of PHFs. The same 4R preparations run on PAGE showed that in the absence of altenusin, the predominant 4R species besides PHFs were monomers, as evident from Coomassie-stained gels (Figure 1C). Western blotting with a 4R-specific antibody additionally
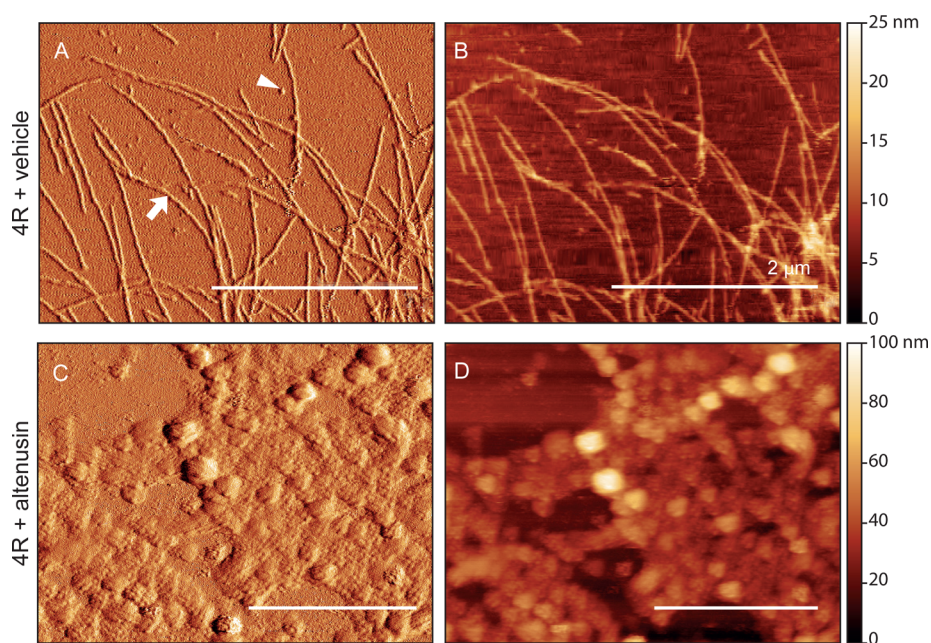
Figure 2. Altenusin induces formation of globular 4R structures. Peak force error and height micrographs of 4R (A, B) and 4R in the presence of altenusin (C, D). (A) 4R fibrils (arrows) and oligomers (arrowheads) induced by heparin after 21 h at 37 °C. (C) In the presence of altenusin, 4R forms globular structures instead of fibrils and oligomers. Representative images from three independent experiments were shown. Scale bar represents 2 μm.

revealed low amounts of dimers and higher order oligomers (Figure 1D). Surprisingly, in the presence of altenusin, there were reduced levels of 4R monomers accompanied by increased levels of dimers and higher order oligomers (Figure 1C and D), suggesting stabilization of intermediate sized tau species. We furthermore found that altenusin induced oxidization of tau, as revealed by reduced iodoacetamide-Oregon Green binding (Figure 1E). Atomic force microscopy (AFM) revealed mostly elongated helical fibrils (5−10 nm) and some large oligomers formed by 4R tau in the absence of altenusin (Figure 2A and B), consistent with ThT assays (Figure 1B). In the presence of altenusin, however, no oligomers or fibrils were observed. Instead, larger globular structures (10−80 nm) were formed by 4R (Figure 2C and D). Taken together, these data suggest that altenusin prevents the formation of large 4R oligomers and fibrils, and instead induces the formation of distinct globular 4R structures.

Next, we tested altenusin in a cell culture model of tau pathology.[15,36] Cells were treated with the protein phosphatase 2A inhibitor okadaic acid to induce pronounced phosphorylation of tau, including at pathological sites Ser396/Ser404 (PHF-1) and Ser422 (pS422), which are closely associated with the formation of NFTs.[17] Treatment of the cells with 10 μM of altenusin markedly reduced phosphorylation of tau by 51 ± 14% at the pS422 epitopes (Figure 3). In AD, tau pathology contributes to disease progression by spreading from neurons of affected brain regions to connected neurons in unaffected brain areas.[19] Although the molecular mechanism of tau pathology spread remains incompletely understood,[21] it has been modeled by incubating cells with PHF tau preparations to induce intracellular tau pathology.[22] Here, fibrillized 4R was added to the culture medium of mature primary hippocampal mouse neurons (Figure 4A) to induce a neuritic tau pathology, visualized by staining of endogenous mouse tau phosphorylated at Ser214, a phosphorylation site of tau that resides outside of the 4R sequence (Figure 4C), While neurons cotreated with 1
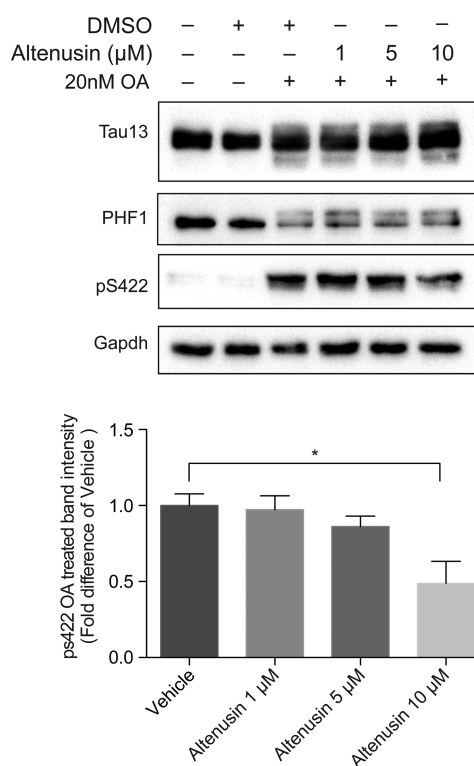

Figure 3. Altenusin reduces tau phosphorylation in SH-SY5Y cells. Okadaic acid treatment of SH-SY5Y cells that stably express human P301L mutant tau (tau13) induces pronounced phosphorylation at serine (S) 396/S404 and S422 (lane 3). Altenusin at 10 μM reduced phosphorylation of tau. Graph: Quantification of the band intensities from five independent experiments (*$P \leq 0.05$).

μM and 10 μM altenusin showed an overall reduction in neuritic staining of phosphorylated Ser214 tau (1 < 10 μM), some pathology remained (Figure 4D and E). In contrast,
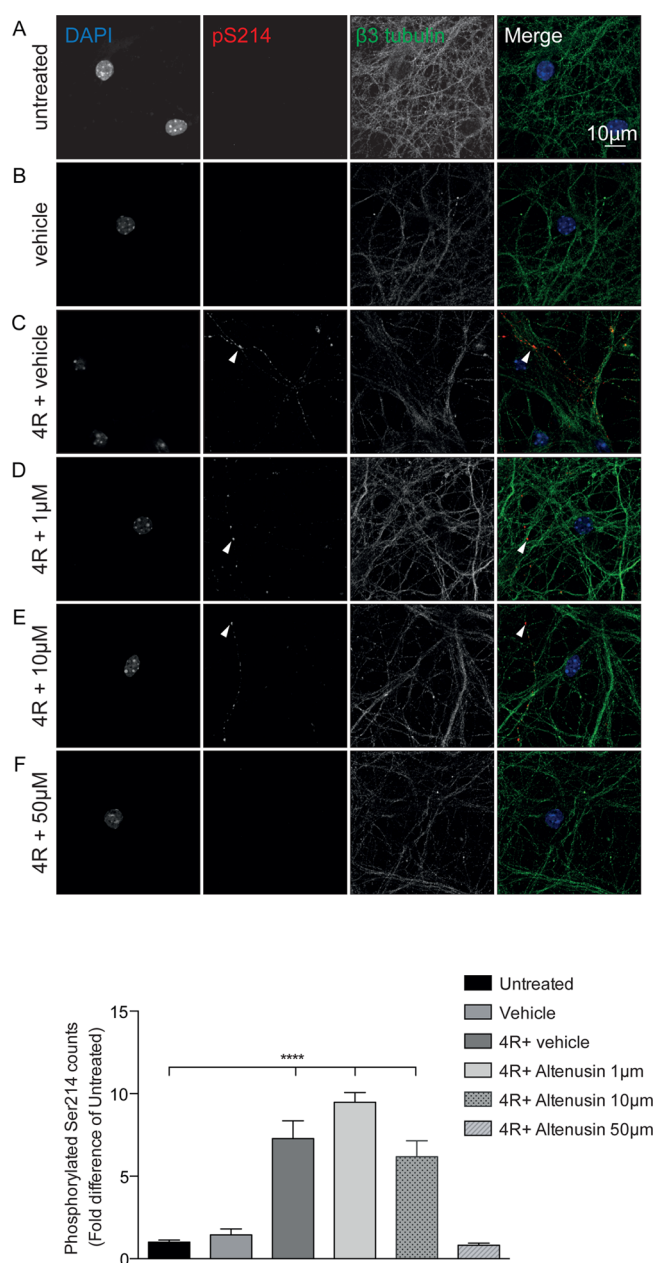
Figure 4. Altenusin reduces induced tau pathology in primary mouse hippocampal cells. Tau phosphorylation was induced in primary mouse hippocampal cells by treating them for 5 days with vehicle (DMSO) (B), 5 μM fibrillised 4R plus vehicle (C), or 5 μM fibrillized 4R in combination with altenusin at 1 μM (D), 10 μM (E), or 50 μM (F). Untreated cells as shown in (A). Counter staining of the neurons for phosphorylation at Ser214 (ps214) show dose-dependent decrease in the levels of neuritic tau phosphorylation (arrowheads). Graph: Quantification of pS214 fluorescence intensities ($n = 10$, ****$P \leq 0.0001$).

neuritic tau phosphorylation epitope Ser214 was absent in cells treated with 50 μM altenusin (Figure 4F). Taken together, altenusin reduced tau phosphorylation and prevented neuritic tau pathology induced by exogenous fibrillized tau in primary neurons. It remains to be shown if these effects are mediated by preventing tau aggregation or via alternative pathways.

Any therapeutic effects of altenusin in vivo were tested by treating TAU58/2 mice, that express P301S mutant tau and show high levels of hyperphosphorylated tau by 3 months as

well as early onset motor and behavioral deficits,[24,37] with altenusin for 10 weeks, starting at 5 weeks of age. Notably, it is very common for mutant tau transgenic mice to display motor and behavioral deficits as major phenotypes, rather than memory deficits.[21,38] These phenotypes should be considered surrogate readouts of neuronal dysfunction and have been utilized for testing drugs in previous studies by others and us.[15] Body weights of TAU58/2 treated with either altenusin or vehicle (DMSO) were comparable (Figure 5A). Next, we subjected altenusin treated and untreated TAU58/2 mice to a series of behavioral paradigms; in the open field arena, the distance traveled was similar, but the time spent in the inner zone were reduced in altenusin- and vehicle-treated TAU58/2 compared to nontransgenic control mice (Figure 5B). Similarly, time spent and distance traveled in the open arm of the elevated plus maze were comparably increased in altenusin- and vehicle-treated TAU58/2 compared to nontransgenic mice (Figure 5C). Both altenusin- and vehicle-treated TAU58/2 mice required the same increased time to descend from the vertical pole during pole testing (Figure 5D). On the accelerating mode RotaRod, both altenusin and vehicle-treated TAU58/2 mice fell off earlier than nontransgenic mice (Figure 5E). The number of slips and time to cross a narrow beam were increased, although not significantly different, in altenusin- and vehicle treated TAU58/2 mice compared to nontransgenic controls (Figure 5F). Following the behavioral testing, we analyzed altenusin- and vehicle-treated TAU58/2 mouse brains for changes in neuropathology, but found no differences in tau pathology assessed by immunofluorescence staining with tau phosphorylation site-specific antibodies against Ser214 and Ser422, NFTs stained by Gallyas silver and tau pathology-associated neurofilament pathology between altenusin- and vehicle-treated TAU58/2 mice (Figure 5G). Taken together, treatment with 2 mg/kg altenusin 3 time a week for a total of 10 weeks did neither improve functional deficits nor reduce NFT neuropathology in TAU58/2 mice.

Antiaggregation treatments targeting tau have entered a new stage with Rember, a methylene blue (MB) compound. Rember is now in phase 3 clinical trials in frontotemporal dementia and AD, following promising results in a phase 2 trial where it slowed disease progression in mild to moderate AD.[39] Interestingly, the effects of MB on tau pathology in different animal models of disease have been inconsistent. While MB reduced tau aggregation in some mouse and *Caenorhabditis elegans* models of tau pathology,[26,28] it failed to prevent tau aggregation in a zebrafish and other mouse models of tau pathology.[29,30,32] Nevertheless, the favorable effects seen in clinical trials highlight targeting fibrillization and aggregation of tau as a valid therapeutic intervention.

Paired helical filament formation is driven by polymerization of tau into β-sheet conformation, resulting in the growth of oligomers and eventually fibrils. Hence, tau-targeted aggregation inhibitors are aimed at interfering with the formation of β-sheets. Accordingly, MB modifies cysteine residues in tau, rendering it incapable of aggregating and forming β-sheets, and instead stabilizes tau's monomeric unstructured form.[33] Using a ThT fibrilization assay, we found that altenusin had similar effects as MB at preventing tau aggregation. However, AFM revealed that tau forms globular structures in the presence of altenusin, and SDS-PAGE showed stabilization of lower order oligomers rather than monomers. Taken together, this suggests alternative mechanisms for aggregation inhibition mediated by MB and altenusin. Interestingly, Ehrnhoefer and colleagues
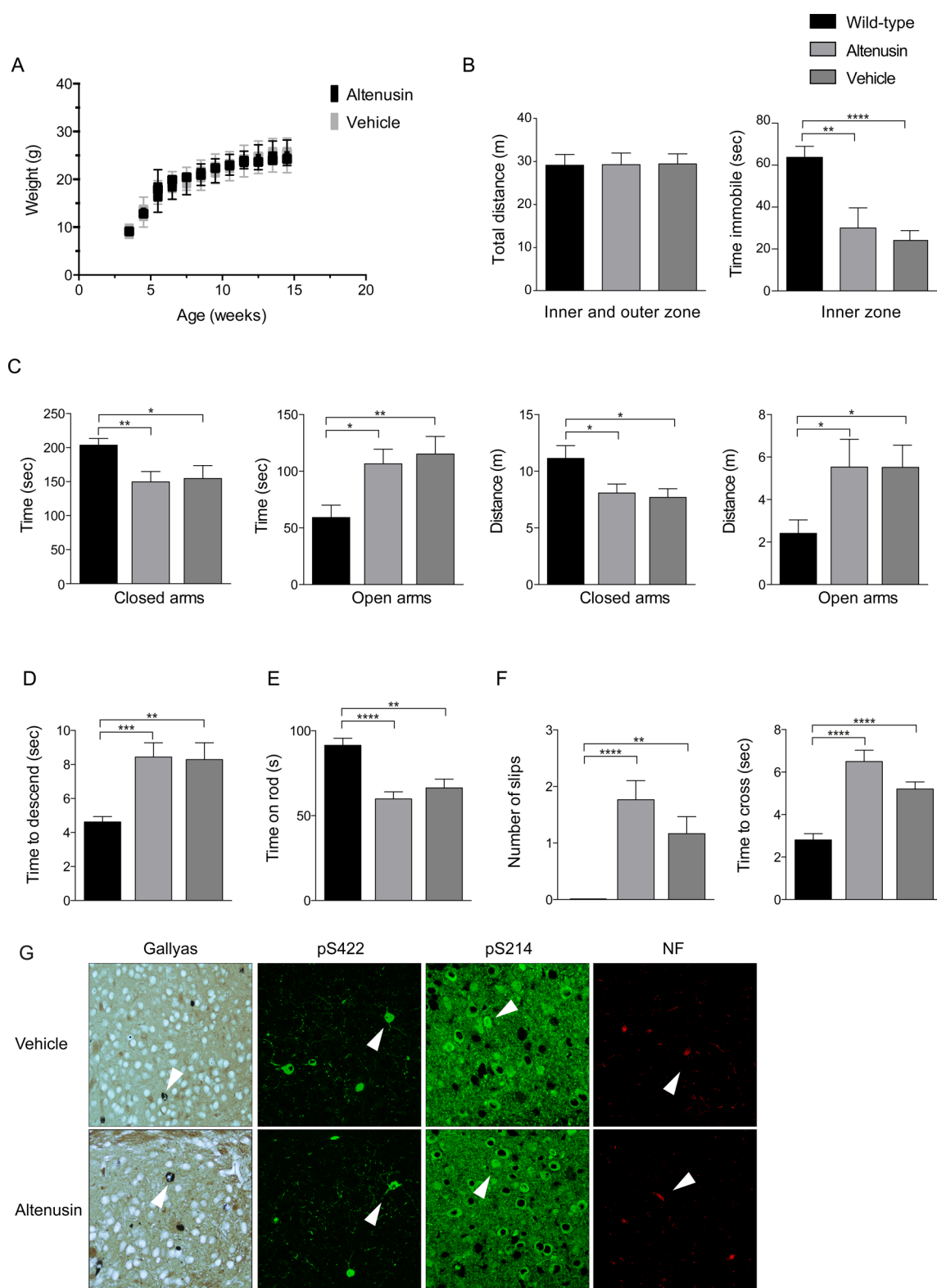
Figure 5. Effects of altenusin on TAU58/2 mice in vivo. (A) Body weight development of altenusin or vehicle treated mice showed no differences. (B-E) Behavioral and motor studies in (B) open field, (C) elevated plus maze, (D) pole test, (E) rotarod, and (F) beam test showed similar performance of altenusin- and vehicle (DMSO)-treated TAU58/2, and oberall reduced performance compared to nontransgenic littermates ($n = 10$ mice per group, $*P \leq 0.05$, $**P \leq 0.01$, $***P < 0.001$, $****P \leq 0.0001$). (G) Representative Gallyas staining of NFTs, tau phosphorylated at S422 (pS422, green) and S214 (pS214, green), and neurofilament (NF, red), in altenusin- and vehicle-treated TAU58/2 mice show no difference in pathology.

reported a polyphenolic compound, (−)-epigallocatechin gallate, which prevents fibrillogenesis of α-synuclein and amyloid-β, but instead drives the formation of unstructured, globular and nonamyloidogenic oligomers.[40] Similarly, altenu-

sin promotes tau to form lower oligomers that present as globular structures and at the same time inhibits tau from forming fibrils. Interestingly, we found that altenusin induced marked oxidization of tau. Oxidization of tau has been proposed as a mechanism by which known inhibitors of tau aggregation, including methylene blue and aminothienopyridazines, prevent fibrilization.[41] If oxidization of tau induced by altenusin directly contributes to the formation of globular tau structures remains to be shown. Given the modulatory role of tau's N- and C-terminus on aggregation, it might furthermore be interesting to determine whether altenusin, or other antiaggregation drugs, have differential effects on distinct tau isoforms.

Phosphorylation of tau at both physiological and additionally at pathological sites is a key event in the development of tau pathology, as it disrupts tau's ability to interact with microtubules and induces conformational changes that make tau prone to aggregation.[34] Therefore, kinase inhibition has been considered as a potential therapeutic approach to targeting tau pathology.[16] Aly and colleagues extracted 15 polyphenolic compounds from *Alternaria* sp., including altenusin, and tested them for inhibitor activity with 24 different protein kinases.[36] Altenusin showed inhibitory effects on 18 kinases, including Src kinase. Although the tested kinases did not include classical tau kinases, such as GSK-3β, cdk5 and MAPK, we decided to determine if altenusin is effective in preventing tau phosphorylation in a cellular model of tau pathology. Consistent with a possible inhibition of specific tau kinases, we found that phosphorylation of tau at the pathological site S422 but not at S396/S404 was reduced in altenusin-treated SH-SY5Y neuroblastoma cells expressing human P301L mutant tau, without affecting total tau levels detected by the Tau13 antibody. An alternative mechanism is that altenusin may change the conformation of tau such that it becomes a less suitable substrate for kinase-mediated phosphorylation at distinct sites. The specific mechanism by which altenusin reduces tau phosphorylation and whether it involves a dual mode of action on tau pathology (i.e., antiaggregation and antiphosphorylation) necessitates subsequent studies in this area.

Using a cell culture model of tau-induced tau phosphorylation, which is a likely step in spread of tau pathology in AD,[42] we found that higher doses of altenusin prevented the formation of neuritic foci containing phosphorylated tau. It remains to be shown if this is due to altenusin disrupting the tau fibrils used for induction, thereby making them ineffective to induced tau phosphorylation in target cells, or due to a kinase-inhibiting function of altenusin as suggested by our experiments in SH-SY5Y cells. Notably, while tau oligomers are understood to confer toxicity,[43] altenusin-induced changes to tau did not result in increased toxicity despite the stabilization of tau oligomers, suggesting a unique signature of these induced structures.

Although altenusin showed efficacy in vitro and in cell culture models, we failed to show a therapeutic benefit in TAU58/2 mice during a 10-week treatment trial, with indistinguishable functional deficits and neuropathology between treated and untreated mice. This may have several reasons, including that altenusin's structure may not be fully optimal to successfully cross the BBB when administered systemically despite a calculated logP 2.4.[44] An alternative explanation could be that altenusin was rapidly degraded during first-pass metabolism and therefore no therapeutic dosages were achieved in the brain. Using different pathogenic mutations in cell culture (P301L) and mice (P301S) is unlikely to be a confounding factor, since mouse lines with different mutations result in comparable pathologies.[21,38] Further extensive studies will be required to identify more precise reasons, other confounding factors and a possible therapeutic potential.

A number of compounds have been previously isolated from bacteria and fungi that successfully inhibit tau aggregation. For instance, quinone derivatives display aggregation inhibitory activity on tau both in vitro and in cells.[27,45] Similarly, we reported previously that fluvic acid inhibits tau aggregation in vitro.[25] Although this present study adds altenusin to the list of potential natural products targeting tau fibrillization, our initial trials in a mouse model of AD with mutant tau expression lends uncertainty as to the validity of its therapeutic use.

■ METHODS

Altenusin Extraction and Isolation. *Penicillium* sp. CVAL4 was isolated from sediment from the South Pacific Ocean, Chile, and was cultivated at 25 °C and 220 rpm for 15 days in CYA medium. The culture broth was then extracted with ethyl acetate to afford 380 mg of a crude broth extract after removal of solvent under reduced pressure. This extract was separated into six fractions (FR1 to FR6) by flash chromatography on C-18 silica using a step gradient method of elution employing water and methanol as solvent systems. The fraction FR4 (60% methanol) was further purified over a Sephadex HL-20 column with methanol as eluent to obtain altenusin. The identity of this compound was confirmed by comparing with existing NMR data.[46] The purified altenusin was used for initial in vitro aggregation experiments. Further to the initial extraction of altenusin, purified material was sourced directly from Santa Cruz at the highest purity available (sc-202454, lot number h1215; purity ≥ 97%, determined by HPLC) for in vitro, and all cell culture and animal experiments.

Protein Expression and Purification. The tau fragment 4R (htau$_{244-372}$) was cloned into pET-28a vector (Novagen) to produce a His-tagged protein in *Escherichia coli* strain BL21 (DE3) as described.[25] 4R tau was isolated from 1 mM IPTG-induced cell lysates using a Talon fast flow column that was eluted with 150 mM of imidazole. Purity of the protein was verified on a Coomassie Brilliant Blue stained SDS-polyacrylamide gel. The concentration of purified 4R was determined using the extinction coefficient at 280 nm (1520 M^{-1} cm^{-1}). The protein was concentrated and stored at −80 °C until use.

Atomic Force Microscopy. Atomic force microscopy (AFM) measurements were performed on a Bruker BioScope Catalyst atomic force microscope with a NanoScope V controller. The probes used were ScanAsyst-Fluid+, with a silicon nitride cantilever and silicon tip. The probes had a nominal spring constant, resonant frequency, and tip radius of 0.7 N/m, 150 kHz, and 2 nm, respectively. Samples were prepared by pipetting 25 μM (30 μL) of protein solution prepared in 10 mM Tris-HCl, pH 7.4 onto freshly cleaved mica substrates and incubated for 20 min at room temperature. The excess protein was removed by washing with the same buffer described above. Mica substrates were placed onto 50 mm glass bottom WillCo-dishes for support. Images were acquired using NanoScope Version 8.15r3 with ScanAsyst mode in fluid at a typical scan rate of 0.8 Hz and data resolution of 256 × 256 or 512 × 512. The peak force set point and gain were adjusted manually to compensate for thermal drift and maintain good tracking of the sample. Each image was line corrected and scar corrected using Gwyddion 2.31. All experiments were carried out in the Biomedical Imaging Facility of the University of New South Wales.

Thioflavin T Fluorescence Assay. The thioflavin T (ThT) fluorescence assay examining the inhibition of tau aggregation by compounds was slightly modified compared to previous reports.[14] Briefly, 20 μM 4R tau and 5 μM heparin (average M_r ≈ 15 000) in 100 mM sodium acetate pH 7.0 with or without 100 μM altenusin was incubated for 48 h at 37 °C. Dithiothreitol at 1 mM was added daily.

ThT as 12.5 μM solution was added, and the incubation continued for 1 h at room temperature prior to fluorescence reading. ThT fluorescence spectra were measured on a Fluoromax-4 spectrometer (Horiba Jobin Yvon) equipped with both excitation and emission monochromators. Excitation was at 440 nm, and emission was collected from 450 to 650 nm in 1 nm increments. All experiments were carried out in the Biomedical Imaging Facility of the University of New South Wales.

Oregon Green-Iodoacetamide Thiol Reactivity Assay. 4R tau was labeled with Oregon Green-iodoacetamide (IAA-OG) (Invitrogen) as previously described,[41] with the following modifications. Heparin induced tau (10 μM) fibrillisation was carried out in sodium acetate buffer (pH7), 40 μM heparin, with 10 μM altenusin at 37 °C for 2 h. Controls were prepared in sodium acetate buffer (pH7) and either reduced with 1 mM DTT or oxidized using 20% v/v DMSO at 37 °C for 2 h. The solutions were further incubated with IAA-OG for 30 min at room temperature. The bound proteins were analyzed by SDS-page and visualized using the Alexa 488 settings on a ChemiDocMP system (BioRad). Bands were quantified and analyzed using Fiji software. Protein loading was determined using Coomassie Blue staining.

Cell Culture. Human SH-SY5Y neuroblastoma cells stably expressing human tau together with the pathogenic P301L mutation have been described previously.[15] Cells were cultured for 3 days, before being treated with either 10 or 50 μM altenusin together with 20 nM okadaic acid for 20 h.

Western Blotting. Proteins were extracted from cultured cells using modified RIPA buffer, as previously described.[47] Protein concentrations of all samples fractions were determined via the Bradford assay. Protein extracts were then analyzed by Western blotting as previously described.[24] Antibodies used were: Tau13 [detecting total tau] (Abcam), PHF-1 (P. Davies, Albert Einstein College of Medicine, New York, NY), pS422 (Biosource), and GAPDH (Millipore).

Primary Murine Neuronal Cell Culture and Treatments. Primary hippocampal cultures from C57BL/6 mice were prepared as previously described.[48] For immunocytochemistry, the cells were cultured for 16 days, before being cotreated with aggregated 4R and altenusin (1, 10, or 50 μM) for 5 days and subsequently fixed with 4% paraformaldehyde on Day 21.

Immunocytochemistry. Fixed cells were prepared for immunocytochemistry as previously described.[49] Briefly, cells were permeabilised with 0.1% Triton-X and blocked in 3% goat serum and 2% bovine serum albumin in phosphate buffered saline (PBS). Primary antibodies were against tau phosphorylated at Ser214 (pS214, Abcam) and β3-tubulin (Abcam). Nuclei were visualized with DAPI. Secondary antibodies (1:1000, Invitrogen) were coupled with the fluorochromes Alexa Fluor 488 or 555. Confocal images were taken on the Zeiss LSM 780 microscope using the Plan-Apochromat 100×/1.4 oil DIC M27 objective.

Mice. All animal experiments have been approved by the Animal Ethics Committee of UNSW and were performed in accordance to the statement on animal experimentation issued by the National Health and Medical Research Council of Australia. Male TAU58/2 mice were used in all animal experiments.[24,37] The TAU58/2 line has been maintained on a C57Bl/6 strain for >10 generations. Nontransgenic littermates were used as controls. Mice were held in groups of 3−6 on a 12 h/12 h light dark cycle with access to food and water ad libitum. Mice expressing the transgene were identified by polymerase chain reaction as previously described.[37]

Treatments. Five week-old mice were randomly allocated to receive intraperitoneal injections of either altenusin 2 mg/kg body weight or the equivalent volume of vehicle three times a week for 10 weeks.

Behavioral Testing. All behavioral and motor testing was performed after the final treatment dose. Test protocols are as previously described[24,37] and briefly detailed below.

RotaRod. Motor performance was determined on a five-wheel RotaRod treadmill (Ugo Basile, Gemonio, Italy) in acceleration mode (5−60 rpm) over 120 s. The average of the longest time each mouse remained on the turning wheel out of three sessions was used for analysis.

Challenge Beam. The beam-traversing test was utilized to assess sensorimotor skills. An 18 cm long dowel was placed over a basin of shallow water with a nesting house placed at the far end to motivate crossing. The time to cross and the number of fore and hind limb slips were recorded. The average of the shortest crossing times and corresponding number of slips from three sessions was used for analysis.

Pole Test. The pole test was utilized to assess grip strength and coordination. Mice were placed at the apex of a vertical pole (an 18 cm long dowel, with a diameter of 0.8 cm) facing upward. The time to turn around and descend the pole and reach the ground (all four paws) was measured. The average of the shortest times from three sessions were used.

Elevated Plus Maze. The Elevated Plus maze (Ugo Basile) consists of two open and two closed arms (each 35 cm × 5.5 cm), joined by a central platform (5.5 cm × 5.5 cm), elevated 60 cm above the ground. Mice were acclimatized to the room for 1 h prior to testing, and then placed on the center platform facing an open arm. Movements were recorded on a ceiling mounted video recorder for 5 min and analyzed using the AnyMaze software.

Body Weight. Body weights (in grams) were measured weekly on a balance.

Histology. Mice were anesthetized and transcardially perfused with PBS (pH 7.4). Brains were removed and immersion fixed in 4% paraformaldehyde and then processed in an Excelsior tissue processor (ThermoFisher, Waltham, MA) for embedding in paraffin and coronal sectioned at either 3 μm for immunohistochemistry (IHC) or 8 μm for Gallyas silver staining. IHC procedures are as previously described.[50] Primary antibodies were against human tau (Tau13, Abcam, Cambridge, UK), tau phosphorylated at Ser214 or Ser422 (pS214 and pS422, Abcam), and 200 kDa heavy NF (NF200, Abcam). Gallyas silver staining was carried out using standard protocols.

Statistical Data Analysis. Statistical analysis was performed using the GraphPad Prism 6.0 software. Data are presented as mean ± SEM and analyzed using either Student's t test or two-way ANOVA. Significance was determined as $P < 0.05$.

■ AUTHOR INFORMATION

Corresponding Authors

*E-mail: l.ittner@unsw.edu.au.
*E-mail: alberto.cornejo@unab.cl.

ORCID

Michael Kassiou: 0000-0002-6655-0529
Lev Lewis: 0000-0002-5469-5456
Lars M. Ittner: 0000-0001-6738-3825

Author Contributions

○S.W.C. and A.C. contributed equally to this study. A.C. and L.I designed the study; S.C., A.C., J.E., C.S., I.V., M.C., A.G., A.M., and L.L. performed experiments; S.C, A.C., M.K., R.W., and L.I. analyzed data; S.C., A.C., and L.I. wrote manuscript with input from all authors.

Notes

The authors declare no competing financial interest.

■ REFERENCES

(1) Gotz, J., Ittner, A., and Ittner, L. M. (2012) Tau-targeted treatment strategies in Alzheimer's disease. *Br. J. Pharmacol.* 165 (5), 1246−59.

(2) Grundke-Iqbal, I., Iqbal, K., Tung, Y. C., Quinlan, M., Wisniewski, H. M., and Binder, L. I. (1986) Abnormal phosphorylation of the microtubule-associated protein tau (tau) in Alzheimer cytoskeletal pathology. *Proc. Natl. Acad. Sci. U. S. A.* 83 (13), 4913−7.

(3) Bedin, M., Gaben, A. M., Saucier, C., and Mester, J. (2004) Geldanamycin, an inhibitor of the chaperone activity of HSP90, induces MAPK-independent cell cycle arrest. *Int. J. Cancer* 109 (5), 643−52.

(4) Farias, G., Cornejo, A., Jimenez, J., Guzman, L., and Maccioni, R. B. (2011) Mechanisms of tau self-aggregation and neurotoxicity. *Curr. Alzheimer Res.* 8 (6), 608−14.

(5) Sahara, N., Maeda, S., and Takashima, A. (2008) Tau oligomerization: a role for tau aggregation intermediates linked to neurodegeneration. *Curr. Alzheimer Res.* 5 (6), 591−8.

(6) Cota, B. B., Rosa, L. H., Caligiorne, R. B., Rabello, A. L., Almeida Alves, T. M., Rosa, C. A., and Zani, C. L. (2008) Altenusin, a biphenyl isolated from the endophytic fungus Alternaria sp., inhibits trypanothione reductase from Trypanosoma cruzi. *FEMS Microbiol. Lett.* 285 (2), 177−82.

(7) Berger, Z., Roder, H., Hanna, A., Carlson, A., Rangachari, V., Yue, M., Wszolek, Z., Ashe, K., Knight, J., Dickson, D., Andorfer, C., Rosenberry, T. L., Lewis, J., Hutton, M., and Janus, C. (2007) Accumulation of pathological tau species and memory loss in a conditional model of tauopathy. *J. Neurosci.* 27 (14), 3650−62.

(8) Barghorn, S., Biernat, J., and Mandelkow, E. (2005) Purification of recombinant tau protein and preparation of Alzheimer-paired helical filaments in vitro. *Methods Mol. Biol.* 299, 35−51.

(9) Oddo, S., Vasilevko, V., Caccamo, A., Kitazawa, M., Cribbs, D. H., and LaFerla, F. M. (2006) Reduction of soluble Abeta and tau, but not soluble Abeta alone, ameliorates cognitive decline in transgenic mice with plaques and tangles. *J. Biol. Chem.* 281 (51), 39413−23.

(10) Sawaya, M. R., Sambashivan, S., Nelson, R, Ivanova, M. I., Sievers, S. A., Apostol, M. I., Thompson, M. J., Balbirnie, M., Wiltzius, J. J., McFarlane, H. T., Madsen, A. O., Riekel, C., and Eisenberg, D. (2007) Atomic structures of amyloid cross-beta spines reveal varied steric zippers. *Nature* 447 (7143), 453−7.

(11) Khlistunova, I., Biernat, J., Wang, Y., Pickhardt, M., von Bergen, M., Gazova, Z., Mandelkow, E., and Mandelkow, E. M. (2006) Inducible expression of Tau repeat domain in cell models of tauopathy: aggregation is toxic to cells but can be reversed by inhibitor drugs. *J. Biol. Chem.* 281 (2), 1205−14.

(12) Meng, S. R., Zhu, Y. Z., Guo, T., Liu, X. L., Chen, J., and Liang, Y. (2012) Fibril-forming motifs are essential and sufficient for the fibrillization of human Tau. *PLoS One* 7 (6), e38903.

(13) Holmes, C., Boche, D., Wilkinson, D., Yadegarfar, G., Hopkins, V., Bayer, A., Jones, R. W., Bullock, R., Love, S., Neal, J. W., Zotova, E., and Nicoll, J. A. (2008) Long-term effects of Abeta42 immunisation in Alzheimer's disease: follow-up of a randomised, placebo-controlled phase I trial. *Lancet* 372 (9634), 216−23.

(14) Friedhoff, P., Schneider, A., Mandelkow, E. M., and Mandelkow, E. (1998) Rapid assembly of Alzheimer-like paired helical filaments from microtubule-associated protein tau monitored by fluorescence in solution. *Biochemistry* 37 (28), 10223−30.

(15) van Eersel, J., Ke, Y. D., Liu, X., Delerue, F., Kril, J. J., Gotz, J., and Ittner, L. M. (2010) Sodium selenate mitigates tau pathology, neurodegeneration, and functional deficits in Alzheimer's disease models. *Proc. Natl. Acad. Sci. U. S. A.* 107 (31), 13888−93.

(16) Brunden, K. R., Trojanowski, J. Q., and Lee, V. M. (2009) Advances in tau-focused drug discovery for Alzheimer's disease and related tauopathies. *Nat. Rev. Drug Discovery* 8 (10), 783−93.

(17) Gotz, J., Chen, F., van Dorpe, J., and Nitsch, R. M. (2001) Formation of neurofibrillary tangles in P301l tau transgenic mice induced by Abeta 42 fibrils. *Science* 293 (5534), 1491−5.

(18) Bulic, B., Pickhardt, M., Schmidt, B., Mandelkow, E. M., Waldmann, H., and Mandelkow, E. (2009) Development of tau aggregation inhibitors for Alzheimer's disease. *Angew. Chem., Int. Ed.* 48 (10), 1740−52.

(19) Braak, H., and Braak, E. (1995) Staging of Alzheimer's disease-related neurofibrillary changes. *Neurobiol. Aging* 16 (3), 271−8 discussion 278−84..

(20) Porat, Y., Abramowitz, A., and Gazit, E. (2006) Inhibition of amyloid fibril formation by polyphenols: structural similarity and aromatic interactions as a common inhibition mechanism. *Chem. Biol. Drug Des.* 67 (1), 27−37.

(21) Ittner, L. M., and Gotz, J. (2011) Amyloid-beta and tau - a toxic pas de deux in Alzheimer's disease. *Nat. Rev. Neurosci.* 12 (2), 65−72.

(22) Frost, B., Jacks, R. L., and Diamond, M. I. (2009) Propagation of tau misfolding from the outside to the inside of a cell. *J. Biol. Chem.* 284 (19), 12845−52.

(23) Peterson, D. W., George, R. C., Scaramozzino, F., LaPointe, N. E., Anderson, R. A., Graves, D. J., and Lew, J. (2009) Cinnamon extract inhibits tau aggregation associated with Alzheimer's disease in vitro. *J. Alzheimer's Dis.* 17 (3), 585−97.

(24) van Eersel, J., Stevens, C. H., Przybyla, M., Gladbach, A., Stefanoska, K., Chan, C. K., Ong, W. Y., Hodges, J. R., Sutherland, G. T., Kril, J. J., Abramowski, D., Staufenbiel, M., Halliday, G. M., and Ittner, L. M. (2015) Early-onset axonal pathology in a novel P301S-Tau transgenic mouse model of frontotemporal lobar degeneration. *Neuropathol. Appl. Neurobiol.* 41 (7), 906−25.

(25) Cornejo, A., Jimenez, J. M., Caballero, L., Melo, F., and Maccioni, R. B. (2011) Fulvic acid inhibits aggregation and promotes disassembly of tau fibrils associated with Alzheimer's disease. *J. Alzheimer's Dis.* 27 (1), 143−53.

(26) Hosokawa, M., Arai, T., Masuda-Suzukake, M., Nonaka, T., Yamashita, M., Akiyama, H., and Hasegawa, M. (2012) Methylene blue reduced abnormal tau accumulation in P301L tau transgenic mice. *PLoS One* 7 (12), e52389.

(27) Pickhardt, M., Gazova, Z., von Bergen, M., Khlistunova, I., Wang, Y., Hascher, A., Mandelkow, E. M., Biernat, J., and Mandelkow, E. (2005) Anthraquinones inhibit tau aggregation and dissolve Alzheimer's paired helical filaments in vitro and in cells. *J. Biol. Chem.* 280 (5), 3628−35.

(28) Fatouros, C., Pir, G. J., Biernat, J., Koushika, S. P., Mandelkow, E., Mandelkow, E. M., Schmidt, E., and Baumeister, R. (2012) Inhibition of tau aggregation in a novel Caenorhabditis elegans model of tauopathy mitigates proteotoxicity. *Hum. Mol. Genet.* 21 (16), 3587−603.

(29) van Bebber, F., Paquet, D., Hruscha, A., Schmid, B., and Haass, C. (2010) Methylene blue fails to inhibit Tau and polyglutamine protein dependent toxicity in zebrafish. *Neurobiol. Dis.* 39 (3), 265−71.

(30) Spires-Jones, T. L., Friedman, T., Pitstick, R., Polydoro, M., Roe, A., Carlson, G. A., and Hyman, B. T. (2014) Methylene blue does not reverse existing neurofibrillary tangle pathology in the rTg4510 mouse model of tauopathy. *Neurosci. Lett.* 562, 63−8.

(31) Dickey, C. A., Kamal, A., Lundgren, K., Klosak, N., Bailey, R. M., Dunmore, J., Ash, P., Shoraka, S., Zlatkovic, J., Eckman, C. B., Patterson, C., Dickson, D. W., Nahman, N. S., Jr., Hutton, M., Burrows, F., and Petrucelli, L. (2007) The high-affinity HSP90-CHIP complex recognizes and selectively degrades phosphorylated tau client proteins. *J. Clin. Invest.* 117 (3), 648−58.

(32) O'Leary, J. C., 3rd, Li, Q., Marinec, P., Blair, L. J., Congdon, E. E., Johnson, A. G., Jinwal, U. K., Koren, J., 3rd, Jones, J. R., Kraft, C., Peters, M., Abisambra, J. F., Duff, K. E., Weeber, E. J., Gestwicki, J. E., and Dickey, C. A. (2010) Phenothiazine-mediated rescue of cognition in tau transgenic mice requires neuroprotection and reduced soluble tau burden. *Mol. Neurodegener.* 5, 45.

(33) Akoury, E., Pickhardt, M., Gajda, M., Biernat, J., Mandelkow, E., and Zweckstetter, M. (2013) Mechanistic basis of phenothiazine-driven inhibition of Tau aggregation. *Angew. Chem., Int. Ed. 52* (12), 3511−5.

(34) Alonso, A. C., Grundke-Iqbal, I., and Iqbal, K. (1996) Alzheimer's disease hyperphosphorylated tau sequesters normal tau into tangles of filaments and disassembles microtubules. *Nat. Med. 2* (7), 783−7.

(35) Raz, Y., Adler, J., Vogel, A., Scheidt, H. A., Haupl, T., Abel, B., Huster, D., and Miller, Y. (2014) The influence of the DeltaK280 mutation and N- or C-terminal extensions on the structure, dynamics, and fibril morphology of the tau R2 repeat. *Phys. Chem. Chem. Phys. 16* (17), 7710−7.

(36) Aly, A. H., Edrada-Ebel, R., Indriani, I. D., Wray, V., Muller, W. E., Totzke, F., Zirrgiebel, U., Schachtele, C., Kubbutat, M. H., Lin, W. H., Proksch, P., and Ebel, R. (2008) Cytotoxic metabolites from the fungal endophyte Alternaria sp. and their subsequent detection in its host plant Polygonum senegalense. *J. Nat. Prod. 71* (6), 972−80.

(37) Przybyla, M., Stevens, C. H., van der Hoven, J., Harasta, A., Bi, M., Ittner, A., van Hummel, A., Hodges, J. R., Piguet, O., Karl, T., Kassiou, M., Housley, G. D., Ke, Y. D., Ittner, L. M., and Eersel, J. (2016) Disinhibition-like behavior in a P301S mutant tau transgenic mouse model of frontotemporal dementia. *Neurosci. Lett. 631*, 24−9.

(38) Ittner, L. M., Halliday, G. M., Kril, J. J., Gotz, J., Hodges, J. R., and Kiernan, M. C. (2015) FTD and ALS-translating mouse studies into clinical trials. *Nat. Rev. Neurol. 11* (6), 360−366.

(39) Wischik, C., and Staff, R. (2009) Challenges in the conduct of disease-modifying trials in AD: practical experience from a phase 2 trial of Tau-aggregation inhibitor therapy. *J. Nutr., Health Aging 13* (4), 367−9.

(40) Ehrnhoefer, D. E., Bieschke, J., Boeddrich, A., Herbst, M., Masino, L., Lurz, R., Engemann, S., Pastore, A., and Wanker, E. E. (2008) Wanker, E. E., EGCG redirects amyloidogenic polypeptides into unstructured, off-pathway oligomers. *Nat. Struct. Mol. Biol. 15* (6), 558−66.

(41) Crowe, A., James, M. J., Lee, V. M., Smith, A. B., 3rd, Trojanowski, J. Q., Ballatore, C., and Brunden, K. R. (2013) Aminothienopyridazines and methylene blue affect Tau fibrillization via cysteine oxidation. *J. Biol. Chem. 288* (16), 11024−37.

(42) Ballatore, C., Lee, V. M., and Trojanowski, J. Q. (2007) Tau-mediated neurodegeneration in Alzheimer's disease and related disorders. *Nat. Rev. Neurosci. 8* (9), 663−72.

(43) Sahara, N., and Avila, J. (2014) "Tau oligomers," what we know and what we don't know. *Front Neurol 5*, 1.

(44) Ghose, A. K., Herbertz, T., Hudkins, R. L., Dorsey, B. D., and Mallamo, J. P. (2012) Knowledge-Based, Central Nervous System (CNS) Lead Selection and Lead Optimization for CNS Drug Discovery. *ACS Chem. Neurosci. 3* (1), 50−68.

(45) Miethbauer, S., Gaube, F., Mollmann, U., Dahse, H. M., Schmidtke, M., Gareis, M., Pickhardt, M., and Liebermann, B. (2009) Antimicrobial, antiproliferative, cytotoxic, and tau inhibitory activity of rubellins and caeruleoramularin produced by the phytopathogenic fungus Ramularia collo-cygni. *Planta Med. 75* (14), 1523−5.

(46) Nakanishi, S., Toki, S., Saitoh, Y., Tsukuda, E., Kawahara, K., Ando, K., and Matsuda, Y. (1995) Isolation of myosin light chain kinase inhibitors from microorganisms: dehydroaltenusin, altenusin, atrovenetinone, and cyclooctasulfur. *Biosci., Biotechnol., Biochem. 59* (7), 1333−5.

(47) van Eersel, J., Ke, Y. D., Gladbach, A., Bi, M., Gotz, J., Kril, J. J., and Ittner, L. M. (2011) Cytoplasmic accumulation and aggregation of TDP-43 upon proteasome inhibition in cultured neurons. *PLoS One 6* (7), e22850.

(48) Fath, T., Ke, Y. D., Gunning, P., Gotz, J., and Ittner, L. M. (2008) Primary support cultures of hippocampal and substantia nigra neurons. *Nat. Protoc. 4* (1), 78−85.

(49) Ittner, A., Chua, S. W., Bertz, J., Volkerling, A., van der Hoven, J., Gladbach, A., Przybyla, M., Bi, M., van Hummel, A., Stevens, C. H., Ippati, S., Suh, L. S., Macmillan, A., Sutherland, G., Kril, J. J., Silva, A. P., Mackay, J., Poljak, A., Delerue, F., Ke, Y. D., and Ittner, L. M. (2016) Site-specific phosphorylation of tau inhibits amyloid-beta toxicity in Alzheimer's mice. *Science 354* (6314), 904−908.

(50) van Eersel, J., Bi, M., Ke, Y. D., Hodges, J. R., Xuereb, J. H., Gregory, G. C., Halliday, G. M., Gotz, J., Kril, J. J., and Ittner, L. M. (2009) Phosphorylation of soluble tau differs in Pick's disease and Alzheimer's disease brains. *J. Neural Transm 116* (10), 1243−51.